

EFFECT OF THE DENSITY OF TWINNING DISLOCATIONS ON THE CONFIGURATION OF STRESS FIELDS NEAR A WEDGE TWIN WITH DIFFERENT SHAPES OF THE BOUNDARIES

O. M. Ostrikov

UDC 536.24

The effect of changes in density of twinning dislocations on one boundary of the wedge twin on the configuration of the stress fields generated by the latter is considered on the basis of a macroscopic dislocation model. Specific features of violation of symmetry of the stress-field distribution near the wedge twin with different shapes of the boundaries are demonstrated for the case of different densities of twinning dislocations on the twin boundaries.

Key words: wedge twin, macroscopic dislocation model, density of twinning dislocations.

A macroscopic dislocation model of a wedge twin was proposed in [1]. This model allows the stress fields inside the twin to be calculated, in contrast to the known model of a thin twin [2]. The model can also take into account both the shapes of the wedge-twin boundaries and the specific features of the distribution of twinning dislocations on the boundaries. Modeling of crystal twinning processes is currently considered as an important research direction; hence, it seems reasonable to develop the macroscopic dislocation model [1] further.

The objective of the present work is to study how the density of the distribution of twinning dislocations on the twin boundaries affects the configuration of stress fields near the wedge twin. The research is performed in such a scale where the distance between the twinning dislocations can be assumed to be infinitely small.

As was demonstrated in [1], the stress fields near a wedge twin can be determined by the formula

$$\begin{aligned} \sigma_{ij}(x, y) = & \int_0^L \sqrt{1 + (f_1'(x_0))^2} \rho_1(x_0) \sigma_{ij}^{(1,0)}(x, y, x_0) dx_0 \\ & + \int_0^L \sqrt{1 + (f_2'(x_0))^2} \rho_2(x_0) \sigma_{ij}^{(2,0)}(x, y, x_0) dx_0, \end{aligned} \tag{1}$$

where L is the twin length, $f_1(x_0)$ and $f_2(x_0)$ are the functions that describe the shapes of the wedge-twin boundaries (Fig. 1), $\rho_1(x_0)$ and $\rho_2(x_0)$ are the densities of the twinning dislocations on the twin boundaries, and $\sigma_{ij}^{(1,0)}$ and $\sigma_{ij}^{(2,0)}$ are the stresses generated on the twin boundaries by individual dislocations, respectively. For a twin located far from the crystal surface, the stresses $\sigma_{ij}^{(1,0)}$ and $\sigma_{ij}^{(2,0)}$ in the approximation of a homogeneous isotropic medium are determined by the formulas

$$\begin{aligned} \sigma_{xx}^{(1,0)} = & -\frac{\mu b_{\text{edge}}}{2\pi(1-\nu)} \frac{(y - f_1(x_0))[3(x - x_0)^2 + (y - f_1(x_0))^2]}{[(x - x_0)^2 + (y - f_1(x_0))^2]^2}, \\ \sigma_{yy}^{(1,0)} = & \frac{\mu b_{\text{edge}}}{2\pi(1-\nu)} \frac{(y - f_1(x_0))[(x - x_0)^2 - (y - f_1(x_0))^2]}{[(x - x_0)^2 + (y - f_1(x_0))^2]^2}, \end{aligned}$$

Sukhoi State Technical University, Gomel' 246746, Belarus; ostrikov@gstu.gomel.by. Translated from *Prikladnaya Mekhanika i Tekhnicheskaya Fizika*, Vol. 49, No. 5, pp. 199–204, September–October, 2008. Original article submitted April 20, 2007; revision submitted July 13, 2007.

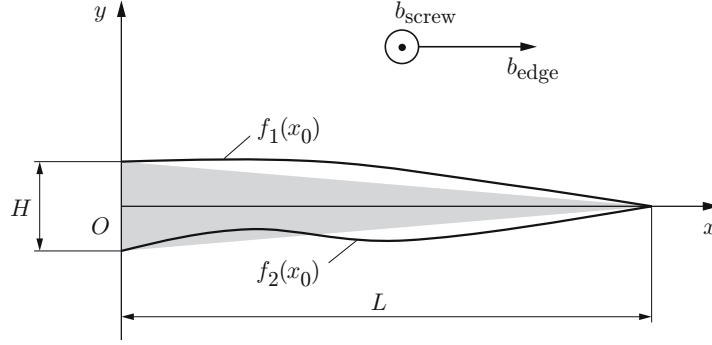


Fig. 1. Schematic of a wedge twin (the dashed region indicates an ideal twin with straight-line boundaries).

$$\begin{aligned}\sigma_{xy}^{(1,0)} &= \frac{\mu b_{\text{edge}}}{2\pi(1-\nu)} \frac{(x-x_0)[(x-x_0)^2 - (y-f_1(x_0))^2]}{[(x-x_0)^2 + (y-f_1(x_0))^2]^2}, \\ \sigma_{zz}^{(1,0)} &= -\frac{\mu b_{\text{edge}}\nu}{\pi(1-\nu)} \frac{y-f_1(x_0)}{(x-x_0)^2 + (y-f_1(x_0))^2}, \\ \sigma_{zx}^{(1,0)} &= -\frac{\mu b_{\text{screw}}}{2\pi} \frac{y-f_1(x_0)}{(x-x_0)^2 + (y-f_1(x_0))^2}, \quad \sigma_{zy}^{(1,0)} = \frac{\mu b_{\text{screw}}}{2\pi} \frac{x-x_0}{(x-x_0)^2 + (y-f_1(x_0))^2}, \\ \sigma_{xx}^{(2,0)} &= -\frac{\mu b_{\text{edge}}}{2\pi(1-\nu)} \frac{(y-f_2(x_0))[3(x-x_0)^2 + (y-f_2(x_0))^2]}{[(x-x_0)^2 + (y-f_2(x_0))^2]^2}, \\ \sigma_{yy}^{(2,0)} &= \frac{\mu b_{\text{edge}}}{2\pi(1-\nu)} \frac{(y-f_2(x_0))[(x-x_0)^2 - (y-f_2(x_0))^2]}{[(x-x_0)^2 + (y-f_2(x_0))^2]^2}, \\ \sigma_{xy}^{(2,0)} &= \frac{\mu b_{\text{edge}}}{2\pi(1-\nu)} \frac{(x-x_0)[(x-x_0)^2 - (y-f_2(x_0))^2]}{[(x-x_0)^2 + (y-f_2(x_0))^2]^2}, \\ \sigma_{zz}^{(2,0)} &= -\frac{\mu b_{\text{edge}}\nu}{\pi(1-\nu)} \frac{y-f_2(x_0)}{(x-x_0)^2 + (y-f_2(x_0))^2}, \\ \sigma_{zx}^{(2,0)} &= -\frac{\mu b_{\text{screw}}}{2\pi} \frac{y-f_2(x_0)}{(x-x_0)^2 + (y-f_2(x_0))^2}, \quad \sigma_{zy}^{(2,0)} = \frac{\mu b_{\text{screw}}}{2\pi} \frac{x-x_0}{(x-x_0)^2 + (y-f_2(x_0))^2}.\end{aligned}$$

Here μ is the shear modulus, ν is Poisson's ratio, and b_{edge} and b_{screw} are the edge and screw components of the Burgers vector of partial twinning dislocations (Fig. 1). All variants of the distribution of twinning dislocations on the twin boundaries and all variants of the shapes of these boundaries are not considered in the present paper. We confine ourselves to studying problems, which are of interest from the viewpoint of physical analysis with allowance for available experimental data on wedge twins.

First, we have to consider twins with straight-line boundaries. Such twins are shaped as extended isosceles triangles and characterize intermediate stages of evolution of twins in a crystal region with a small number of defects [3]. Therefore, an increase in density of twinning dislocations on certain segments of the boundaries of such twins can be considered as a process preceding the twin-boundary curvature, because an increase in the twin width enhances the incoherence of the twin boundary and, as a consequence, increases the density of twinning dislocations on convex segments of the twin boundaries. Vice versa, a decrease in the twin width (for instance, in the case of a concave twin boundary) reduces the density of twinning dislocations on such a boundary or its segment. Therefore, by modeling a decrease or increase in density of twinning dislocations on a straight-line twin boundary, based on the model developed in [1], one can study the stress state near a wedge twin at the stage preceding the curvature of its boundary.

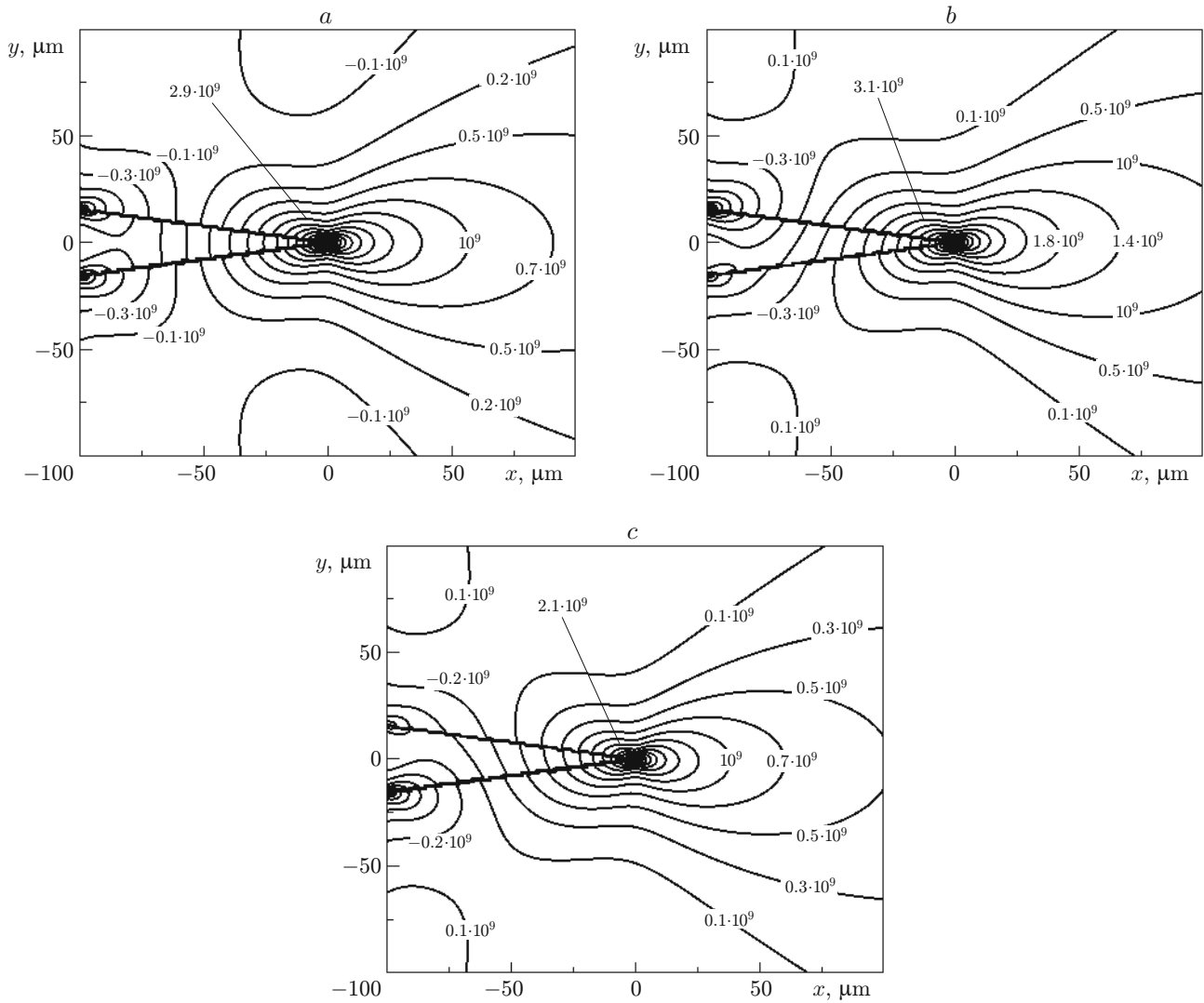


Fig. 2. Distribution of shear stresses η_{xy} near a wedge twin with straight-line boundaries: (a) $\rho_1 = \rho_2 = 0.5 \cdot 10^9 \text{ m}^{-1}$; (b) $\rho_1 = 10^9 \text{ m}^{-1}$ and $\rho_2 = 0.5 \cdot 10^9 \text{ m}^{-1}$; (c) $\rho_1 = 0.25 \cdot 10^9 \text{ m}^{-1}$ and $\rho_2 = 0.5 \cdot 10^9 \text{ m}^{-1}$.

In the case of straight-line boundaries, the functions $f_1(x_0)$ and $f_2(x_0)$ in (1) have the form

$$f_1(x_0) = (H/2)(1 - x_0/L), \quad f_2(x_0) = -(H/2)(1 - x_0/L), \quad (2)$$

where H is the twin width near the twin mouth (see Fig. 1).

For $\rho_1(x_0) = \rho_2(x_0) = \text{const} = \rho$, with allowance for Eq. (2), Eq. (1) yields

$$\sigma_{ij}(x, y) = \rho \sqrt{1 + \left(\frac{H}{2L}\right)^2} \int_0^L (\sigma_{ij}^{(1,0)}(x, y, x_0) + \sigma_{ij}^{(2,0)}(x, y, x_0)) dx_0.$$

Let us illustrate the calculation results by an example of the distribution of shear stresses σ_{xy} . This component of the stress tensor is important for studying the interaction of a wedge twin with edge dislocations. The calculation results are presented in the form of the distribution

$$\eta_{xy}(x, y) = \sigma_{xy}(x, y)/A_{xy},$$

where $A_{xy} = \mu b_{\text{edge}}/[2\pi(1 - \nu)]$, which allows the analysis to be performed regardless of characteristics of particular materials.

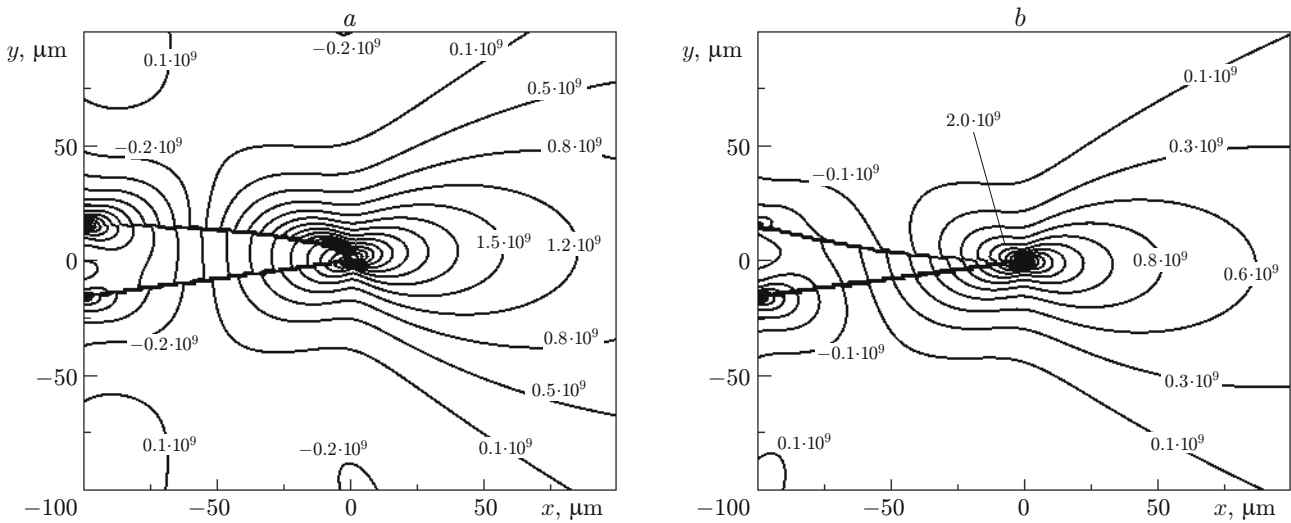


Fig. 3. Distribution of shear stresses η_{xy} near a wedge twin: (a) convex twin boundary ($\rho_1 = 10^9 \text{ m}^{-1}$ and $\rho_2 = 0.5 \cdot 10^9 \text{ m}^{-1}$); (b) concave twin boundary ($\rho_1 = 10^9 \text{ m}^{-1}$ and $\rho_2 = 0.25 \cdot 10^9 \text{ m}^{-1}$).

The order of magnitude of the density of dislocations was estimated on the basis of the experimental data [4–6]. We used the calculated relation

$$\rho = N/L = H/(2aL),$$

where N is the number of twinning dislocations on the twin boundary and a is the parameter of the crystal lattice in the direction perpendicular to the twinning plane. Let us use $H = 31 \text{ }\mu\text{m}$, $L = 100 \text{ }\mu\text{m}$, and $a = 0.31 \text{ nm}$. Then, we obtain $\rho = 0.5 \cdot 10^9 \text{ m}^{-1}$. This value is three orders of magnitude greater than that in the example considered in [7], where the twin length was much greater than its width. Such twins can be described by the thin twin model. The model proposed in the present work can also be applied for twins with a commensurable length and width. Such twins usually have a high density of twinning dislocations on the boundaries.

Figure 2a shows the distribution of shear stresses for the case of identical densities of twinning dislocations on two twin boundaries and the shape of the boundaries described by functions (2). The distribution of the shear stress field is symmetric with respect to the Ox axis. The stress σ_{xy} is positive near the twin apex and negative near the twin mouth. In the middle part of the twin, the shear stress is close to zero.

If the density of twinning dislocations on one boundary is higher than on the other one, the symmetry of the distribution of the shear stress fields considered is violated (Fig. 2b), which precedes the curvature of the twin boundary with a higher density of twinning dislocations. This boundary becomes convex [3], and its profile on the xOy plane is described by the function

$$f_1(x_0) = (H/2)\sqrt{1 - (x_0/L)^2}. \quad (3)$$

The shear stresses calculated with the use of Eq. (3) for an excess density of twinning dislocations on the curved boundary are plotted in Fig. 3a. Intense deformations of the crystal often lead to the emergence of new twins on the convex boundary and to branching of already existing twins [8].

The symmetry of the distribution of stresses σ_{xy} is also violated if the number of twinning dislocations on the twin boundary is reduced (see Fig. 2c). This violation precedes the formation of a concave twin boundary whose profile is described by the function

$$f_1(x_0) = (H/2)(x_0^2/L^2 - 2x_0/L + 1).$$

The shear stress distribution for a concave twin boundary is shown in Fig. 3b.

It is reasonable to define the curvature of the twin boundaries in the initial conditions because the shape of the twin boundaries depends not only on the field of internal stresses in the crystal, but also on the difference in the generation rates of twinning dislocations on the twin boundaries. The differences in the generation rates may

be caused, for instance, by a gradient of external stresses near the twin mouth in the direction perpendicular to the twin development direction. The stresses generated by the twin proper are of interest in this case.

Thus, the effect of the density of twinning dislocations on the twin boundaries on the stress field configuration calculated on the basis of a macroscopic dislocation model near a wedge twin with different shapes of the boundaries is studied. A change in density of twinning dislocations on one boundary of the twin is found to violate the symmetry of the stress field distribution near the twin.

REFERENCES

1. O. M. Ostrikov, "Macroscopic dislocation model of a wedge twin," *Vestn. Gomel. Gos. Tekh. Univ.*, No. 2, 10–18 (2006).
2. A. M. Kosevich and V. S. Boiko, "Dislocating theory of elastic twinning of crystals," *Usp. Fiz. Nauk*, **104**, No. 2, 101–255 (1971).
3. O. M. Ostrikov, "Some features of wedge-shaped twins in bismuth single crystals deformed by a concentrated load," *Fiz. Met. Metaloved.*, **90**, No. 1, 91–95 (2000).
4. M. V. Klassen-Neklyudova, *Mechanical Twinning of Crystals* [in Russian], Izd. Akad. Nauk SSSR, Moscow (1960).
5. O. M. Ostrikov, "Use of thin polyparaxylene films to study the plastic deformation bismuth single crystals," *J. Appl. Mech. Tech. Phys.*, **47**, No. 4, 596–599 (2006).
6. O. M. Ostrikov and S. N. Dub, "Study of mechanical twinning of antimony single crystals by the method of nano-indentation," *Inzh.-Fiz. Zh.*, **76**, No. 1, 170–172 (2003).
7. A. M. Kosevich, *Dislocations in the Theory of Elasticity* [in Russian], Naukova Dumka, Kiev (1978).
8. O. M. Ostrikov, "Branching of wedge twins in bismuth single crystals deformed by a concentrated load," *Fiz. Met. Metaloved.*, **87**, No. 1, 94–96 (1999).